RSC Advances

Assessment of iron ore mineral wastes for sulfate removal from groundwater wells: A case study

Journal:	*RSC Advances*
Manuscript ID	RA-ART-10-2015-021843.R1
Article Type:	Paper
Date Submitted by the Author:	27-Dec-2015
Complete List of Authors:	Sadeghalvad, Bahareh; Amirkabir University of Technology, department of Mining & Metallurgical Engineering, Amirkabir University of Technolog Azadmehr, Amirreza; Department of Mining and Metallurgical Engineering , Amirkabir University of Technology Hezarkhani, Ardeshir ; Amirkabir University of Technology,, department of Mining & Metallurgical Engineering, Amirkabir University of Technology,
Subject area & keyword:	Materials < Physical

Assessment of iron ore mineral wastes for sulfate removal from groundwater wells: A case study

B.Sadeghalvad[1], A.Azadmehr[2]*, A.Hezarkhani[3]

Department of Mining & Metallurgical Engineering, Amirkabir University of Technology, Tehran, Iran

1- PhD candidate in department of Mining & Metallurgical Engineering, Amirkabir University of Technology, Tehran, Iran, B_sadeghalvad@aut.ac.ir, address: Amirkabir University of Technology, 424 Hafez Avenue, Tehran, Iran, 1875-4413. Phone: 00989132123126.

2- Assistance professorindepartment of Mining & Metallurgical Engineering, Amirkabir University of Technology, Tehran, Iran. A_azadmehr@aut.ac.ir, address: Amirkabir University of Technology, 424 Hafez Avenue, Tehran, Iran, 1875-4413. Phone: 00989124195819.

3- Professorofdepartment in Mining & Metallurgical Engineering, Amirkabir University of Technology,Tehran, Iran. Ardehez@aut.ac.ir address: 424 Hafez Avenue, Tehran, Iran, 1875-4413. Phone: 00982164542968.

Assessment of iron ore mineral wastes for sulfate removal from groundwater wells: A case study

Abstract

To reduce environmental risks of mining activities, it is important to find out eco-friendly efficiency of mine waste. One way to utilize mine waste is to reuse them as an adsorbent in environmental decontamination. This study describes the efficiency of Choghart iron ore mineral wastes (namely Quartz-Albitophire and Metasomatic) as an efficient adsorbent of sulfate decontaminated groundwater wells of Bafq district in the center of Iran. At first, iron ore mineral waste were characterized by XRD, XRF, FTIR spectroscopies and petrographic observations of thin sections. The main parameters such as pH, contact time, initial sulfate concentration and amount of adsorbent have been optimized for maximum sulfate removal, by the response surface methodology (RSM) based on the central composite design (CCD) method. Based on RMS analysis, the sulfate removal models proved a good agreement with the experimental values, by very low probability values (<0.0001). From the predicted model, maximum sulfate adsorption onto Metasomatic and Quartz-Albitophire were 31.07 and 20.27 mg/g, respectively. This adsorption rate indicates that the seemingly worthless iron ore mineral waste can be useful to eliminate one of the most hazardous environmental pollution. To identify the mechanism of adsorption, the equilibrium of adsorption process were examined by non-linear isotherm models (Langmuir, Frendlich, Temkin, D-R, Redlich-Peterson, Toth and Koble–Corrigan). These studies uncovered that the sulfate adsorption onto Quartz-Albitophire has a complex treatment, and it seems the combinations of heterogeneous and homogenous adsorption occur on the surface. The heterogeneous sulfate adsorption onto Metsomatic has been confirmed by Toth and Koble-Corigan models. According to optimum conditions of sulfate adsorption, the maximum removed amounts of sulfate from Bafq groundwater wells using Quartz-Albitophire and Metasomatic were 29.33 and 15.62 mg/g, respectively.

Keywords: Iron ore waste, adsorbent, Sulfate, Decontamination, Equilibrium isotherm.

1. Introduction

The main source of drinking water and irrigation is groundwater wells which can be contaminated with natural and anthropogenic sources. One of the toxic species in groundwater, which should be alleviated from ecosystem, is sulfur compounds in different types of RSH, R_2S, HS^-, S^{2-}, SO_3^{2-} and SO_4^{2-} forms, from which some can be converted into sulfite and sulfate by oxidative processes. Sulfate in drinking water has a permissible amount of 250 mg/L[1]. If sulfate contents exceeds acceptable limit, it will lead to an unpleasant bitter taste of domestic water, plumbing corrosion, and more significantly in humans, the concentrations of 500 to 750 mg/L cause a laxative effect, catharsis, dehydration and gastrointestinal irritation [2]. Efficient removal of sulfate from water is a complicated issue due to its high solubility, high oxidation number and stability in aqueous solutions. Various treatment techniques have been used for sulfate removal including reverse osmosis[3], electro dialysis, ion exchange, chemical precipitation[4] and biological methods. Generally, there are plenty of drawbacks with these methods like: high capital, operational cost, problems in disposal of the residual metal sludge and limited removal efficiency.

Adsorption is one of the most efficient process for sulfate removal, especially by natural adsorbents, due to its noticeable lower costs, easy handling and abundant in nature[5-14]. A summary of amount of sulfate adsorption onto natural adsorbents are presented in Table.1. This research has focused on the investigation of mine waste efficiency as an adsorbent of environmental pollution. The reason for choosing iron ore mineral wastes as an adsorbent of sulfate is that these wastes can be a combination of different materials which play a role as an adsorbent for sulfate uptake from solution. As typical iron ore waste contains minerals, such as Feldspar, Quartz, Iron oxide and Aluminum oxide which could potentially be used as an adsorbent of sulfate ions from solution [1516-2021, 22].

In this study, the Bafq district in Yazd province in the center of Iran was chosen for water decontamination by affordable iron ore mineral waste adsorbent. The aims of this study are: 1) to evaluate the performance of iron ore mineral waste for sulfate removal from aqueous solution, 2) to investigate the optimum condition to achieve the maximum amount of adsorption and 3) to identify the mechanism of sulfate adsorption onto iron ore waste.

To achieve this goal, after identifying characteristics of iron ore waste, the experiments have been done on synthetic sulfate solution to obtain the optimum conditions of adsorption onto selected iron waste, such as Metasomatic and Quartz-Albitophire and the following experiments have been performed to found sulfate adsorption mechanism onto adsorbents by equilibrium isotherm models and finally sulfate removal process from groundwater wells of Bafq area has been studied.

Table 1. A summary of amount of sulfate adsorption onto natural adsorbents.

2. Study Area

The studied area is located in Bafq district in Yazd province (Fig.1), which is a part of the Central Iranian microplate in the Alpine-Himalayan orogenic system.

Fig. 1. The map of study area.

2.1 The contaminated groundwater wells in Bafq (Adsorbate)

Due to arid ecosystem and importance of water resources crises in the center of Iran, water reclamation has intensively gained attention. Thirty water wells which are mainly hosted by clays and sands (Fig. 2), were used for the sampling of water. As seen in Table 2, Electrical conductivity (EC), total dissolved solid (TDS) and pH and sulfate (SO_4^{2}) were measured.

Fig. 2. The map depicts study area in center of Iran and the location of Choghart mine and water wells in the area.

The mean value of sulfate ion in these groundwater wells are much more than the permissible amount (Table 2). In this study, to investigate the efficiency of considered adsorbent for sulfate removal, the water of four groundwater wells, i.e. 1: Sadrabad well, 2: Bagherabad well, 3: Ghavidel well and 4: Slamabad well, which are shown in Fig 2 have been examined after consideration the effect of different parameters in sulfate adsorption process.

Table 2. Statistical summary of the chemical species from samples in the studied area

2.2 Choghart iron ore mineral waste

The Choghart iron mine (55°28′2″E, 31°42′00″N) is located in 12 km northeast of Bafq town in the center of Iran. Mineralization at this mine occurs mainly with a high-grade iron ore (magnetite and hematite), a high phosphorous-low grade iron, Metasomatic and Quartz-Albitophire rocks (Fig.3). The Metasomatic and Quartz-Albitophire are the part of mine waste rocks which in this study are considered as an adsorbent of sulfate.

Fig.3. Simplified geological map of the ore body of the Choghart deposit (pit face 2011).

Quartz-Albitophire which is located in the north side of the Choghart mine (Fig. 3) shows sharp contact with iron ore (Hematite) in northeastern of the Choghart iron mine (Fig. 4). Metasomatic rocks are located in the south side of mine which are spread from east to west.

Fig. 4. The Choghart iron deposit. a) A panorama showing part of the northeastern ore body. b) Sharp contact between the Quartz-Albitophire (Altered rhyolite) host rock and the iron ore.

3. Experimental

3.1. Material and physical instruments

Quartz-Albitophire and Metasomatic of Bafq area was used without any chemical pretreatment and modification as the adsorbent. The samples were ground and sieved by ASTM standard sieves to obtain the nominal particle size of -150 μm in diameter. Sulfate-contaminated groundwater was well provided by the water wells of Bafq district, in the center of Iran. The pH of the aqueous phase was monitored using a pH meter (Fisher Scientific pH meter). Initial pH of solution was adjusted by HCl and NaOH solutions (5 M) .In order to characterize the samples the X-ray diffraction (XRD) patterns of the samples were recorded in an Philips X-ray diffract meter using CuKα radiation. The composition of samples were examined by Philips X-ray fluorescence (XRF) using X-ray diffractmeter Xunique II) with Cu Ka radiation Fourier transform infrared (FTIR) spectrum from were recorded on a Shimadzu IR instrument, Sulfate concentrations were measured by Unicam UV-Visible spectrophotometer at λ_{max} = 420 nm.

3.2. Experimental design

The response surface methodology (RSM) is an efficient technique for the optimization of sulfate adsorption [23], thus RSM method based on central composite design (CCD), which is the most frequently used form of RSM[23], was used to investigate the effect of four variables by design expert 9 (DX9) statistical software. This method determined the effectiveness of parameters and identified the optimum operation conditions.

The total number of experiments for each adsorbent was 30, including16 factorial points (2^4), 8 axial points (2*4) and 6 central points. The factors (variables) were coded according to the following equation[24]:

$$x_i = \frac{X_i - X_{io}}{\Delta X_i} \qquad (1)$$

Where x_i is the coded value of the i_{th} independent variable, X_i is the natural value of the i_{th} independent variable, Xi_o is the natural value of the i_{th} independent variable at the central point, and ΔXi is the step change value.

Table 3. Range of values of CCD for adsorption of sulfate onto Quartz-Albitophire

In order to fit the experimental results of CCD, a second-order (quadratic) polynomial equation was used as follows:

$$y = b_0 + \sum_{i=1}^{k} b_i x_i + \sum_{i=1}^{k} b_{ii} x_i^2 + \sum_{1 \le i \le j}^{k} b_{ij} x_i x_j + e \qquad (2)$$

Where y is the predicted response, k is the number of variables, b_0 is the constant term, b_i, b_{ii} and b_{ij} represents the coefficients of the linear, quadratic and interaction parameters respectively, x_i represents the variables, and symbol e is the residual associated to the experiments[25].

In order to evaluate the proposed model and to study the effect of variables, the analysis of variance (ANOVA) was applied. ANOVA is based on partitioning of the whole variability of

data (SS_T) into its components parts related to the main effects of each factor (SS_A, SS_B, …), to their interactions (SS_{AB}, SS_{BC}, …, SS_{ABC}, …) and to the experimental error [26, 27].

$$SS_T = \sum_{i=1}^{n_i} (x_i - \overline{\overline{x}})^2 = SS_A + SS_B + ... + SS_{AB} + SS_{BC} + ... + SS_{ABC} + ... + SS_{ERR} \quad (3)$$

$$SS_{ERR} = \sum_{j=1}^{n_j} (x_j - \overline{x})^2 \quad (4)$$

.

3.3. Equilibrium studies

Isotherm models, indicating the relation between adsorbent and adsorbate in equilibrium, have been studied for sulfate adsorption onto both adsorbents by seven different non-linear isotherm models including two parameter and three parameter models. The non-linear form of equations of these models was represented in Table 4.

Non-linear regression MATLAB software was employed for determination of constant of two and three-parameter models. In addition of correlation coefficient (R^2), to confirm the best fit of isotherm models, the employed error functions were used as follows:

1. A derivative of Marquardt's percent standard deviation (MPSD):

$$\sum_{i=1}^{n} \left[\frac{(q_{e,\exp} - q_{e,calc})}{q_{e,\exp}} \right]_i^2 \quad (5)$$

2. Residual root mean square error (RMSE):

$$\sqrt{\frac{1}{n-2} \sum_{i=1}^{n} (q_{e,\exp} - q_{e,calc})^2} \quad (6)$$

3. The average percentage errors (APE):

$$\frac{\sum_{i=1}^{n}\left|(q_{e,\exp}-q_{e,calc})/\mathrm{q}_{e,\exp}\right|_i}{n}\times 100 \qquad (7)$$

Where $q_{e,exp}$is the experimental data of adsorption, $q_{e,cal}$ is obtained data by calculation from adsorption models and n is number of experimental points [28].

Table4. Non-linear Isotherm equations of different isotherm models.

4. Results and discussion

4.1. Characterization of the adsorbents

4.1.1 Characterization of Quartz-Albitophire

Quartz-Albitophire is a host rock of iron mineral which is located in the north side of Choghart mine The mineralogical study indicates that in the Quartz-Albitophire sample quartz and Albite were the main constituents, where the diffractions appear at 26.60^o and 27.90^o (2θ) correspond to planes (011) and (002) of Albite crystal structure, respectively. The main diffraction of quartz crystal structure is observed at 2θ =26.6^o which corresponds to plane (011) (Fig.5).

According to the amount of elemental analysis of SiO_2, Na_2O and Al_2O_3(Table 5), the Quartz-Albitophire sample contains 50.45 % w/w quartz and 49.55% Albite.

Fig. 5. XRD pattern of Quartz-Albitophire and Metasomatic.

Table 5. Chemical analysis of Quartz-Albitophire and Metasomatic sample (XRF)

The Fourier transform infrared (FTIR) spectrum and band assignments of Quartz-Albitophire and Metasomatic samples are represented in Fig. 6. As mentioned in elemental analysis, the presence of quartz in the Quartz-Albitophire samples can be explained by Si-O asymmetrical bending vibrations in the 463 cm^{-1} and Si-O symmetrical stretching

vibrations in the 787 cm^{-1}[129]. In the range of580-1100 cm^{-1}, Albite shows a large number of peaks. Substitution of Na by K in alkali feldspars causes specific spectral features, especially in the stretching bands between 700 and 800 cm^{-1}[130].The FTIR spectrum for feldspar exhibits the presence of hydroxyl groups (OH vibration band) at 3620.16 cm^{-1}[131].

Fig. 6. FTIR spectrum of Quartz-Albitophire and Metasomatic samples.

Quartz-Albitophire is a host rock of iron mineral which is located in the north side ofChoghart mine. As observed in Fig. 7, Quartz-Albitophire is shown in bright color. As a result of carbonatization and re crystallization, Quartz-Albitophire has a fine grain size and amorphous particles in a granoblastic texture. This host rock consists predominantly of quartz, Plagioclase and Orthoclase. Sericite and mica minerals in this rock are related to the alteration of orthoclase or plagioclase feldspars minerals, which are subjected to hydrothermal alteration (Fig 8.a &b). Opaque minerals (iron oxides) are observed in Fig 8, too.

Fig. 7. The Choghart iron waste rocks. a Quartz-Albitophire and altered rhyolite in bright color and metasomatic in green color. b metasomatic rocks.

Fig. 8. Photomicrographs of Quartz-Albitophire host rock in thin section (XPL). (Chl: Chlorite, Qtz: Quartz, Src: Sericite, Alb: Albite, Fe-Ox: iron oxide, Mic: mica) (50x)

4.1.2 Characterization of Metasomatic sample

Metasomatic mineral is located in the south side of Choghart mine .The mineralogical study indicates that in the Metasomatic sample, Quartz, Diopside and Tremolite were the main constituents (Fig. 5). The diffraction peaks of Tremolite crystal are observed at 10.37^{o}, 28.59^{o} and 33.08^{o} (2θ), which the main peak at 10.37 is corresponded to plane (001). Tremolite and Diopside are overlapped in lots of diffraction peaks, such as 27.65^{o}, 29.96^{o}, 30.37^{o} and 35.12^{o} (2θ). The indicant diffraction peaks for Diopside are appeared at 30.94^{o} and 35.70^{o} (2θ) corresponding to planes(011) and (002).

According to the amount of elemental analysis of SiO_2,CaO, MgO and Al_2O_3 in Metasomatic sample (Table 5) and calculation of silica percentage in Diopside and

Tremolite Metasomatic sample contains 19.33 % w/w quartz, 65.41% w/w Tremolite and 14.58% w/w Diopside.

For Metasomatic sample (Fig. 6), the main vibration band is found in the range of 1100 and 800 cm^{-1}. The presence of shoulder bands at 1100, 1065, 993 and 947 cm^{-1}concern to Si-O-Si asymmetric stretching vibrations which can be belonged to functional groups of feldspar and Termolite – Diopside components. For Termolite and Diopside components the band at 919 cm^{-1}can be attributed to the symmetric stretching vibration of Si-O-Si [32, 33]. The observed band at 3673 $cm^{-1}$is attributed to OH stretching vibrations of Mg-OH or Fe-OH^{+} and the band and 3429 cm^{-1} is indicated OH stretching vibrations of water molecular in the sample [33, 34]. The sharp bands at 457 and 507 $cm^{-1}$are attributed to Si-O-Si asymmetrical bending vibrations of Quartz and Feldspar components respectively.

Metasomatic mineral, which is located in the south side of Choghart mine, is characterized by thin section too. Metasomatic is green in color (Fig.7) and consists predominantly of amphiboles, phyllosilicates and pyroxene minerals. In the low grade alteration of Metasomatite rocks Amphiboles appears as Edenite and in the high grade alteration amphiboles occurs as Tremolite and Actinolite (Fig. 9.a). As shown in Fig. 9.b Talc- Serpentine and Biotite phyllosilicates are observed in Metasomatic samples. The other minerals which can be mentioned in this type of rock are Apatite and Pyroxene (Fig. 9.c.d).

Fig. 9.Photomicrographs of Metasomatic host rock in thin section (XPL). a Actinolitization in the host metasomatic. b Talc-Serpentine and Biotite in host metasomatite. c,d Apatite and pyroxene in host rock. (Act: actinolite; Bio: Biotite; Ser: Serpentine; Pyx: Pyroxene; Ap: apatite).(100X)

4.2. Optimum conditions of sulfate adsorption

In order to determine significant parameters and to find relationship among variable such as pH, contact time, the initial sulfate concentration and amount of adsorbent with other in sulfate adsorption onto Quartz-Albitophireand Metasomatic, statistical design of experiments was

carried out to employ 30 sulfate adsorption experiments for each adsorbent. The results are shown in Table 6 and 7 respectively. The analysis of variance (ANOVA) was used to evaluate the significance of the main effects and interactions of the operating factors on the investigated parameters during sulfate adsorption. Results analysis and the effects of variables of sulfate adsorption onto Quartz-Albitophire and Metasomatic were presented separately.

Table 6. Arrangement of the CCD for variables in sulfate adsorption onto Quartz-Albitophire

Table 7. Arrangement of the CCD for variables in sulfate adsorption onto Metasomatic

4.2.1 Results analysis and the effects of variables of sulfate adsorption onto Quartz-Albitophire

According to ANOVA analysis(Table 8) among evaluated variables (pH, contact time, sulfate initial concentration and amount of adsorbent) in sulfate adsorption onto Quartz-Albitophire, the effects of the initial sulfate concentration(x_3), amount of adsorbent (x_4) and their interaction were statistically significant. Also, pH value with less impact on the sulfate uptake was effective, but contact time and the interactions of other considered variables were statistically insignificant.

The effects of important variables and their interactions are shown in Figure 10. As can be observed Figure 10.a displays the interaction effect between the initial sulfate concentration and amount of Quartz-Albitophire on the sulfate uptake, and Figure 10.b illustrates the interaction effect between the initial sulfate concentration and pH on the sulfate uptake. According to Table 8 and Figure 10, the initial concentration had positive effect on sulfate removal, while amount of adsorbent and pH negatively influenced sulfate removal, however their effect was not as high as initial concentration. The maximum sulfate adsorption was found approximately in the middle of the contact time range.

Figure 11 (a, b) show the predicted sulfate removal values against the actual values and normal plot of residual for sulfate removal. As can be seen in Figure 11.a, the residuals have a normal distribution because the points follow a straight line. Figure11.b shows that the predicted values match the experimental values reasonably well and therefore the results can be predicted by statistical model.

As given in the ANOVA analysis in Table 8, the coefficient of determination (R^2) of sulfate adsorption onto Quartz-Albitophireis 0.972, indicate a satisfactory arrangement of the quadratic model to the experimental data. The coefficient of variance (CV), indicating the percentage of the ratio of the standard error of estimate to the mean value of the observed response is25.85. The predicted sum of squares (PRESS), showing how a particular model fits each point in the design, is 353.24. The adequate precision value, admeasuring the 'signal to noise ratio' and being desirable when this ratio is more than 4, is 22.08[35]. These results proved a satisfactory adjustment of the quadratic model to the experimental data.

Fig. 10.Surface plot of the effects of main variable interaction on the sulfate adsorption onto Quartz-Albitophire, a. Sulfate initial concentration and amount of Quartz-Albitophire, b. sulfate initial concentration and pH

Fig. 11. a) Normal plot of residual for sulfate removal ; b) Relation between experimental and predicted sulfate removal by Quartz-Albitophire.

Table 8. ANOVA Table for Experimental design for sulfate adsorption onto Quartz-Albitophire.

As seen in Table 3, the optimization of sulfate adsorption was carried out by a multiple response method (desirability function)to optimize different combinations of the process parameters, such as pH of solution (x_1), contact time(x_2), sulfate initial concentration (x_3) and amount of adsorbent (x_4).The desirability function equation describing the influence of the factors on the overall desirability was as follows(Eq. 8).:

$$\begin{aligned} Q-Alb: \quad (mg/g)Adsorption = {} & +3.74501 - 0.21939x_1 - 0.01365x_2 \\ & + 0.00667x_3 - 1.12133x_4 + 0.00206x_1x_2 - 0.00051x_1x_3 \\ & + 0.01341x_1x_4 - 0.0000011x_2x_3 - 0.00181x_2x_4 - 0.00115x_3x_4 \\ & - 0.00404x_1^2 + 0.00003x_2^2 + 0.0000045x_3^2 + 0.14821x_4^2 \end{aligned} \tag{8}$$

The sulfate adsorption on any condition in the interval of our experiment design can be calculated from Eq. (8) attentively.

The main aim of this study was to maximize sulfate removal in the adsorption process.

Process optimization has been done by numerical optimization option in design expert software. The proposed desirable experimental condition suggested by software was pH = 2, contact time= 130 min, sulfate initial concentration 1950 mg/L and amount of adsorbent 4 g for 20.27 mg/g sulfate adsorption onto Quartz-Albitophire. By testing the recommended condition, the sulfate removal reaches to 16.47 mg/g, showing good agreement with the value obtained from the model.

4.2.2 Results analysis and the effects of variables of sulfate adsorption onto Metasomatic

The ANOVA analysis of sulfate adsorption onto Metasomatic (Table 9) reveals that the effective variables in sulfate adsorption onto Metasomatic were the effects of sulfate initial concentration(x_3), amount of adsorbent (x_4) and their interaction, which initial sulfate concentration have a positively influenced the adsorption, while the amount of adsorbent had negative effect on sulfate adsorption.

The interaction effect between the initial sulfate concentration and pH and the interaction effect between amount of interaction effect and the initial sulfate concentration on the sulfate uptake toward Metsomatic are presented in Figures 12a and 12b, respectively.

Based on Table 7 and Figure 12, the amount of sulfate adsorption in low and high pH was more than neutral pH, although the pH variable did not show any significant trend toward sulfate adsorption. As given in the ANOVA analysis in Table 9, the coefficient of determination (R^2) for Metasomatic is 0.9635, indicating a satisfactory arrangement of the quadratic model to the experimental data. The coefficient of variance (CV)is 33.57, and the predicted sum of squares (PRESS) is 1543.34for Metasomatic. The adequate precision value is 19.71[35].Since the amount of adequate precision was more than 4, the amount of PRESS was high enough and the CV value was less, this model can be used to predict the design attentively.

According to Tables8 and 9, and in comparison with the model considered for sulfate adsorption onto Quartz-Albitophire and Metasomatic, it can be concluded that the adjustment of the predicted quadratic model to the experimental data for the both were satisfactory and calculable.

Based on ANOVA analysis, the initial sulfate concentrations as well as the amount of adsorbent play an important role in the sulfate adsorption for both adsorbents.

Fig.12. Surface plot of sulfate adsorption onto Metasomatic showing interaction between sulfate initial concentration, pH and amount of Metasomatic at the central values of other parameters.

Table 9. ANOVA Table for Experimental design for sulfate adsorption onto metasomatic.

Figures 13 (a, b) shows the predicted sulfate removal values against the actual values and normal plot of residual for sulfate removal by Metasomatic. As van be seen in Figure13.a, the residuals have a normal distribution, since the points follow a straight line. Figure 13.b shows that the predicted values match the experimental values reasonably well and therefore the results can be predicted by statistical model.

Fig. 13. a) Normal plot of residual for sulfate removal,; b) Relation between experimental and predicted sulfate removal by Metasomatic.

The relationship between response and operating parameters (pH(x_1), contact time(x_2), sulfate initial concentration (x_3) and amount of adsorbent (x_4)) for sulfate adsorption onto Metasomatic, can be expressed as a function of operating parameters as Eq. (9).

$$\begin{aligned} \textit{Metasomatic}: \quad q(mg/g) &= 5.25848 - 3.13563x_1 - 0.06389x_2 \\ &+ 0.029739x_3 - 1.94634x_4 - 0.0035413x_1x_2 \\ &- 0.0003226x_1x_3 + 0.15266x_1x_4 - 0.0000149x_2x_3 \\ &+ 0.0091541x_2x_4 - 0.0041138x_3x_4 + 0.23119x_1^2 \\ &+ 0.0003997x_2^2 + 0.0000038x_3^2 + 0.2017700x_4^2 \end{aligned} \qquad (9)$$

This model can be used to calculate, the sulfate adsorption on any condition in the interval of our experiment design attentively.

The proposed optimum condition for sulfate adsorption onto Metasomatic by numerical optimization of software was pH = 2, contact time= 11 min, sulfate initial concentration 1770 mg/L and amount of adsorbent 4 g for 31.07 mg/g amount of adsorption. By testing the recommended condition, the sulfate removal reached to 26.17, which showed good agreement with the value obtained from the model.

Since in the adsorption process with both adsorbent the maximum adsorption occurs in high sulfate initial concentration, it can be concluded that these adsorbents without modification are not favorable in low sulfate concentration but just in high sulfate concentration these adsorbents are good enough for sulfate adsorption.

Suitable ability of Quartz-Albitophire and Metasomatic to remove sulfate from groundwater wells indicate that the seemingly worthless iron ore mineral waste can be useful to eliminate one of the most hazardous environmental pollution.

4.3. Equilibrium studies

The equilibrium results (Fig. 14) for sulfate adsorption by Quartz-Albitophire and Metasomatic were fitted for two parameter and three-parameter models. Constant parameters and values for model validation (R^2 and error functions) were represented in Table 10.The results are as follows:

4.3.1. Equilibrium studies of sulfate adsorption onto Quartz-Albitophire

According to the assumption of different isotherm models represented in Table 4, and due to their constants in Table 10, and by considering two parameter models and their constants, it is concluded that sulfate adsorption process onto Quartz-Albitophire is favorable (Langmuir: $0<R_L<1$ and Freundlich: $0<1/n<1$) and with respect to calculated free energy from Dubinin-Radshkevich model physical interaction (E<8 KJ/mol) between sulfate ions and Quartz-Albitophire surface adsorption is dominant. The value of sulfate adsorption capacity which was calculated from Langmuir model is 24 mg/g.

The R^2 value of Langmuir (0.93) is more than Freundlich (0.90) isotherm, however the value of correlation coefficient (R^2) for Langmuir is not acceptable to predict mechanism of sulfate adsorption because it is not so close to unity, therefore to determine mechanism of sulfate adsorption onto Quartz-Albitophire (homogenous or heterogeneous), it is preferred to investigate other isotherm equations as three-parameter models, which can identify the mechanism of adsorption process with more certainly. The sequence of isotherm models considering R^2 values is in this order:

Toth>Dubinin-Radshkevich>Temkin>Langmuir>Koble–Corrigan>Freundlich>Redlich Peterson, and the sum of the normalized errors for Marquardt's Percent Standard Deviation (MPSD) and Residual Root Mean Square Error (RMSE) follow this order: Temkin<Toth~ Freundlich<Dubinin-Radshkevich<Redlich-Peterson~ Langmuir<Koble–Corrigan.

Since the lower amount of error functions and the higher amount of R^2 value indicate more correlation between experimental data and calculation data obtained from models, and by combing these two indexes, it can be concluded that sulfate adsorptive behavior onto Quartz-Albitophire is more predictable by Temkin and Toth models. This conclusion is confirmed by

Average Parentage Error (APE), which is lower for Temkin and Toth than other models (Table 10).

Temkin model has modified the Langmuir model by considering the effect of temperature in the adsorption processe.B_T constant of Temkin model, relevant to the heat of adsorption, indicating interaction between sulfate ions and Quartz-Albitophire surface is weak, since the value of B_T is less than 8 KJ/mol[36]. This conclusion confirmed the results obtained from Dubinin-Radshkevich model (physical adsorption process).

Toth model developed the Langmuir isotherm model to improve the fitting experimental data and predicted values by the assumption of a quasi-Gussian energy as a binding energy between adsorbate and adsorbent. Toth model is applicable to heterogeneous adsorption[37-39].

On the one hand, Toth model, which is represented heterogeneous adsorption, is fitted better than other models to experimental data. Of course Langmuir model, implying to monolayer adsorption is fitted better than Freundlich isotherm, but the study of three-parameter models imply that the combination of heterogeneous and homogenous adsorption can be possible for sulfate adsorption onto Quartz-Albitophire. According to Toth model, which has a closest fit to the equilibrium experimental data even better than Langmuir model the adsorption of sulfate onto Quartz-Albitophir eintends to heterogeneous adsorption.

However, more than one mechanism for sulfate adsorption process onto Quartz-Albitophire shows that the adsorption process is complex since adsorbent (Quartz-Albitophire) isthe composition of quartz and Albite which have different adsorption behavior.

4.3.2. Equilibrium studies of sulfate adsorption onto Metasomatic

According to Table 10, the values of constants of Langmuir, Freundlich, Temkin and D-R models for sulfate adsorption onto Metasomatic showed that the adsorption mechanism was a favorable (Langmuir: $0<R_L<1$ and Freundlich: $0<1/n<1$) and physical ($E<8$) adsorption with 28.51mg/g maximum monolayer adsorption capacity.

Of course, all of error functions emphasize that Freundlich model is the best model to explain adsorption behavior of Metasomatic toward sulfate ions, however R^2(0.94) values for this model is not good enough to decide absolutely about adsorption mechanism of sulfate uptake, thus investigating isotherm model adsorption by three-parameter models is reasonable. The sequence

of isotherm model considering R^2 value follows this order: Koble–Corrigan>Toth>Freundlich>Langmuir >Temkin>Redlich-Peterson >Dubinin-Radshkevich. According to the sum of the normalized errors for Marquardt's Percent Standard Deviation (MPSD) and Residual Root Mean Square Error (RMSE), this sequence is predominate: Koble–Corrigan ~Toth<Freundlich<Langmuir<Temkin<Redlich-Peterson <Dubinin-Radshkevich. The sequence of models, considering the Average Parentage Error (APE) is similar to the mentioned order. Thus, the closest fit to the equilibrium experimental data is relevant to Koble-corrigan, Toth and Freundlich models. All these three models imply heterogeneous mechanism of adsorption. Therefore, sulfate adsorption onto Metasomatic was done in a heterogeneous surface with a non- uniform distribution of heat of adsorption.

Table10. Isotherm model constants for sulfate adsorption onto Quartz-Albitophire and Metasomatic.

4.3.3. Comparative equilibrium studies of Quartz-Albitophire and Metasomatic as an adsorbent of sulfate

Sulfate adsorption process onto Quartz-Albitophire and Metasomatic shared many similarities. They were similar in the apparent energy of adsorption (K_L coefficient in Langmuir were close to each other), adsorption intensity (n coefficient in Freundlich were close to each other), adsorption capacity (K_F coefficient of Freundlich are close to each other), heat of adsorption (similar B_T coefficient in Temkin) and physical adsorption mechanism (E<8 D-R in both adsorbent). Heterogeneous uptake was dominant for sulfate adsorption process onto both adsorbents. The only difference was that the adsorption of sulfate onto Quartz-Albitophire was done in combination of heterogeneous and homogenous adsorption.

Fig. 14. Isotherm plots for sulfate adsorption onto a. Quartz-Albitophire and b. Metasomatic.

4.4. Adsorption mechanism

As observed in Isotherm studies demonstrated that sulfate adsorption process onto Quartz-Albitophire is a complex process by the combination of the heterogeneous and homogenous

uptake. According to the optimum values of Sulfate adsorption onto both adsorbents, pH affects protonation of functional groups (Si-OH or Fe-OH) on the surface that causes a positive charge on the Q-Al and Metasomatic surface. This phenomenon has occurred more on the Metasomatic surface. The species of Sulfate ions in 2 pH is observed as HSO_4^- form. In other words, HSO_4^- is adsorbed on the protonated hydroxyl groups in acidic solution as presented in the following equations:

$$R-OH+H^+ \rightarrow R-OH_2^+ \qquad (R \text{ symbol can be } Al, Si \text{ and } Fe \text{ elements})$$

$$H^+ + SO_4^{2-} \rightarrow HSO_4^-$$

Mechanism adsorption for both adsorbents Q-Al and Metsomatic on acidic solution is suggested:

$$R-OH_2^+ + HSO_4^- \rightarrow R-OH_2^+ ....HSO_4^-$$

According to Temkin and Dubinin-Radushkevich model, this interaction is a weak physical interaction.

4.5. The removal of sulfate from ground water wells of Bafq area

After investigating the efficiency of iron ore mineral wastes (Metasomatic and Quartz-Albitophire) to adsorb sulfate from sulfate synthetic solution, and recognizing the optimum condition of these processes, the removal of sulfate from water wells of Bafq area was investigated. These studies were performed in pH 2, by 4 g adsorbent and contact time 11 minutes and 130 minutes for Metasomatic and Quartz-Albitophire, respectively. In order to remove sulfate from the four wells of Bafq area, experiments carried out, and results are given in Table 11. As illustrated in table 11, the removal of pollution (sulfate) from water wells has increased with increasing sulfate concentration. As obviously observed, there is asynergistic effect of increasing sulfate contamination of groundwater wells.Sincewellno.3, had the highest sulfate pollution, sulfate uptake toward Metasomatic and Quartz-Albitophirewere29.3 and 15.6 mg/g respectively. According to these values the ability of Metasomatic and Quartz-

Albitophirefor removal of sulfate from groundwater are considerable ratios to other mineral adsorbents [5-11].

Table 11. The amount of sulfate adsorption in water wells of Bafq district.

5 Conclusion

1. This paper introduced Iron ore mineral wastes, namely Quartz-Albitophire and Metasomatic as effective and efficient adsorbents to remove sulfate from groundwater wells without any modification. Although Choghart iron ore mineral wastes seem a worthless material, Quartz-Albitophire and Metasomatic can be used to overcome a major environmental problem such as sulfate removal from ground wastewater wells which was proved in this study. In other words, one of the advantages of this study is the use of new processing route to remove environmental pollution by a waste material.
2. Mineralogy of Quartz-Albitophire indicated that it mainly consists of quartz, Plagioclase and Orthoclase. Given the ANOVA analysis, initial sulfate concentration and the amount of Quartz-Albitophire had a significant impact on the process of sulfate adsorption onto Quartz-Albitophire. The maximum amount of adsorption led to 26.2 mg/g in case of 2 pH, 130-min contact time, 1950 mg/L initial sulfate concentration and 4 g amount of adsorbent. According to these optimum conditions, the best adsorption amount of sulfate from water wells was related to No. 3 (Ghavidel well) with uptake of 15.6 mg/g sulfate. This reduction in sulfate uptake from groundwater ratio to synthetic solution can be attributed to competitive adsorption between sulfate and other ions in groundwater. Isotherm studies demonstrated that sulfate adsorption process onto Quartz-Albitophire is a complex process by the combination of the heterogeneous and homogenous uptake. The maximum monolayer adsorption capacity was 24.8 mg/g which was done in a favorable and physical adsorption. With respect to the results of Toth model, sulfate adsorption on the Quartz-Albitophire tends to occur on the heterogeneous surface.
3. The other iron mine waste used as an adsorbent of sulfate was the south mine waste, which is called Metasomatic. It is green in color and predominantly consists of amphiboles, phyllosilicates and pyroxene minerals. By investigating the impacts of various variables on sulfate adsorption onto Metasomatic, the ANOVA analysis

demonstrated that among pH, contact time, initial sulfate concentration and amount of adsorbent, initial sulfate concentration and amount of adsorbent had a significant impact on sulfate adsorption process. According to numerical optimization, the maximum amount of adsorption for sulfate adsorption onto Metasomatic was 31.1 mg/g in 2 pH, 11-min contact time, 1770 mg/L initial sulfate concentration and 4 g amount of adsorbent. According to this optimum conditions for Metasomatic absorbent, the best adsorption quantity of sulfate from water wells was related to No. 3 (Ghavidel well) with uptake of 29.3 mg/g sulfate. This reduction in sulfate uptake from groundwater ratio to synthetic solution can be relevant to competitive adsorption between sulfate and other ions in groundwater. Among the various isotherms tests, the Toth, koble-Corrigan and Freundlich models showed experimental data fit better than other models indicating the heterogeneous adsorption by Metsomatic.

.

Acknowledgment

The authors would like to acknowledge Geological Survey of Iran (G.S.I) for providing samples of groundwater wells from Bafg area.

References

1. W. H. Organization, *Geneva, Switzerland*, 2006, 366.
2. L. Chien, H. Robertson and J. Gerrard, *Canadian Medical Association Journal*, 1968, **99**, 102.
3. W. Pulles, G. Juby and R. Busby, *Water Science & Technology*, 1992, **25**, 177-192.
4. D. Feng, C. Aldrich and H. Tan, *Minerals Engineering*, 2000, **13**, 623-642.
5. T. Delfosse, P. Delmelle and B. Delvaux, *Geoderma*, 2006, **136**, 716-722.
6. M. Ishiguro and T. Makino, *Colloids and Surfaces A: Physicochemical and Engineering Aspects*, 2011, **384**, 121-125.
7. M. Ishiguro, T. Makino and Y. Hattori, *Journal of colloid and interface science*, 2006, **300**, 504-510.
8. M. Pigna and A. Violante, *Communications in soil science and plant analysis*, 2003, **34**, 2099-2113.
9. S. M. Rao and A. Sridharan, *Clays Clay Miner*, 1984, **32**, 414-418.
10. M. Alves and A. Lavorenti, *Geoderma*, 2004, **118**, 89-99.
11. T. Sokolova and S. Alekseeva, *Eurasian Soil Science*, 2008, **41**, 140-148.
12. S. Koumaiti, K. Riahi, F. Ounaies and B. Ben Thayer, *Journal of Environmental Science and Engineering*, 2011, **5**, 1570-1580.
13. A. Moret and J. Rubio, *Minerals Engineering*, 2003, **16**, 715-722.

14. C. Namasivayam and D. Sangeetha, *Desalination*, 2008, **219**, 1-13.
15. N. Priyantha and S. Perera, *Water resources management*, 2000, **14**, 417-434.
16. N. Y. Acelas, S. M. Mejia, F. Mondragón and E. Flórez, *Computational and Theoretical Chemistry*, 2013, **1005**, 16-24.
17. K. Fukushi, K. Aoyama, C. Yang, N. Kitadai and S. Nakashima, *Applied Geochemistry*, 2013, **36**, 92-103.
18. U. Rafique, A. Imtiaz and A. K. Khan, *Journal of Water Sustainability*, 2012, **2**, 233-244.
19. P. Roonasi and A. Holmgren, *Journal of colloid and interface science*, 2009, **333**, 27-32.
20. M. Zhu, P. Northrup, C. Shi, S. J. Billinge, D. L. Sparks and G. A. Waychunas, *Environmental Science & Technology Letters*, 2013, **1**, 97-101.
21. L. Charlet, N. Dise and W. Stumm, *Agriculture, ecosystems & environment*, 1993, **47**, 87-102.
22. C.-H. Wu, S.-L. Lo and C.-F. Lin, *Colloids and Surfaces A: Physicochemical and Engineering Aspects*, 2000, **166**, 251-259.
23. M. Vaez, A. Zarringhalam Moghaddam and S. Alijani, *Industrial & Engineering Chemistry Research*, 2012, **51**, 4199-4207.
24. I.-H. Cho and K.-D. Zoh, *Dyes and Pigments*, 2007, **75**, 533-543.
25. M. A. Bezerra, R. E. Santelli, E. P. Oliveira, L. S. Villar and L. A. Escaleira, *Talanta*, 2008, **76**, 965-977.
26. M. Gharabaghi, M. Irannajad and A. R. Azadmehr, *Environmental Engineering and Management Journal*, 2014, **13**, 2963-2970.
27. A. Bose, *Factorial Design of Experiments, Examples & Exercises*, BIMTECH, 2009.
28. M. Hadi, M. R. Samarghandi and G. McKay, *Chemical engineering journal*, 2010, **160**, 408-416.
29. V. Ramasamy, P. Rajkumar and V. Ponnusamy, *Indian Journal of Physics*, 2009, **83**, 1295-1308.
30. D. Feng, J. L. Provis and J. S. Deventer, *Journal of the American Ceramic Society*, 2012, **95**, 565-572.
31. H. Ismail, H. Osman and A. Ariffin, *Polymer-Plastics Technology and Engineering*, 2005, **43**, 1323-1344.
32. N. Gopal, K. Narasimhulu and J. Rao, *Spectrochimica Acta Part A: Molecular and Biomolecular Spectroscopy*, 2004, **60**, 2441-2448.
33. E. Izci, *LPI Contributions*, 2014, **1783**, 5049.
34. A. Pacella, G. Andreozzi and J. Fournier, *Chemical Geology*, 2010, **277**, 197-206.
35. Q. K. Beg, V. Sahai and R. Gupta, *Process Biochemistry*, 2003, **39**, 203-209.
36. R. Huang, B. Wang, B. Yang, D. Zheng and Z. Zhang, *Desalination*, 2011, **280**, 297-304.
37. F. Gimbert, N. Morin-Crini, F. Renault, P.-M. Badot and G. Crini, *Journal of Hazardous Materials*, 2008, **157**, 34-46.
38. A. Günay, E. Arslankaya and İ. Tosun, *Journal of Hazardous Materials*, 2007, **146**, 362-371.
39. M. Zhang, H. Zhang, D. Xu, L. Han, D. Niu, B. Tian, J. Zhang, L. Zhang and W. Wu, *Desalination*, 2011, **271**, 111-121.

Table 1. A summary of amount of sulfate adsorption onto natural adsorbents.

Adsorbent	Q_m(mg/g)	Ref.
Andisols	15.36	(Pigna and Violante, 2003)
	13.44	(Delfosse et al., 2006)
	24	(Ishiguro and Makino, 2011)
	28.8	(Ishiguro et al., 2006)
Kaolinite	1.2	(Rao and Sridharan, 1984)
soils of the Sao Paulo State, Brazil	0.74	(Alves and Lavorenti, 2004)
chitin-based shrimp shells	156	(Moret and Rubio, 2003)
coconut coir pith	4.9	(Namasivayam and Sangeetha, 2008)
Raw Date Palm Seeds	3.2	(Koumaiti et al., 2011)

Table 2.Statistical summary of the chemical species from samples in the studied area

Variables	Mean	Minimum	Maximum
SO_4^{2-}(mg/l)	2796.83	201.7	6266.6
Cl^-(mg/l)	3278.21	146	6804.8
TDS (g/l)	100.59	2.07	1035
pH	7.43	6.92	8.16
EC (mS/cm)	138.99	2.07	1983

Table 3. Range of values of CCD for adsorption of sulfate onto Quartz-Albitophire.

Adsorbent	Variables	Symbol	Code variable levels				
			-1.1	-1	0	+1	+1.1
Quartz-Albitophire	pH	x_1	1.6	2	6	10	10.4
	t (min)	x_2	9	20	130	240	251
	C_0 (mg/L)	x_3	110	200	1100	2000	2090
	Amount of adsorbent (g)	x_4	0.7	1	4	7	7.3
Adsorbent	Variables	Symbol	Code variable levels				
			-1.2	-1	0	+1	+1.2
Metasomatic	pH	x_1	1.2	2	6	10	10.8
	t (min)	x_2	1	10	55	100	109
	C_0 (mg/L)	x_3	75	250	1125	2000	2175
	Adsorbent Amount (g)	x_4	1.5	2	4.5	7	7.5

Table 4. Non-linear Isotherm equations of different isotherm models.

models	Non-linear Equation	Descriptions	Hypotheses	Ref
Two parameter:				
Langmuir	$q_e = \frac{q_m k_L C_e}{1 + k_L C_e}$ $R_L = \frac{1}{1 + k_L C_0}$	q_m Maximum adsorption capacity (mg/g); K_L Adsorption intensity or Langmuir coefficient (L/mg). R_L separation factor.	• Monolayer adsorption; • The adsorbent is homogeneous; • All sites are identical and energetically equivalent • $0<R_L<1$ is favorable.	(Gimbert et al. , 2008)
Freundlich	$q_e = K_F C_e^{1/n}$	K_F relative adsorption capacity ($mg^{1-1/n} L^{1/n} g^{-1}$);nadsorption intensity	• Multilayer adsorption; • Adsorption onto heterogeneous surfaces; • Reversible adsorption. • $0<1/n<1$ is favorable.	(Gimbert et al. , 2008)
Temkin	$q_e = \frac{RT}{B_T} \ln(A_T C_e)$	A_T and $B_T$temkin constant that B_T is related to the heat of adsorption (J/mol); R gas constant (8.314 J/molK) T absolute temperature (K)	• The fall in the heat of adsorption is linear rather than logarithmic; • Investigate the heat of adsorption.	(Gimbert et al. , 2008; Günay et al. , 2007)
Dubinin-Radushkevich	$q_e = q_{\max} \exp(\frac{\varepsilon^2}{-2E^2})$ $\varepsilon = \mathrm{RT} \ln(1 + 1/\mathrm{C}_e)$	E: free energy per molecule of adsorbate (KJ/mol)	• Energy of Adsorption: E<8 : physical adsorption, 8<E<16 : chemical absorption or ion exchange E>16: particle diffusion governs the reaction	(Günay et al. , 2007)
Three parameter:				
Redlich-Peterson	$q_e = \frac{K_{RP} C_e}{1 + a_{RP} C_e^g}$	K_{RP} (L/g)and a_{RP}(L/mg) Redlich-Peterson constants; g Redlich-Petersonexponent	• Applied in homogeneous or heterogeneous systems • limiting behaviors: g=1 Langmuir form g=0 Henry's law form	(Gimbert et al. , 2008; Günay et al. , 2007)
Toth	$q_e = \frac{q_m b_T C_e}{[1 + (b_T C_e)^{1/n_T}]^{n_T}}$	K_TToth maximum adsorption capacity (mg/g), a_TToth equilibrium constant	• Langmuir-based isotherm • Applicable to heterogeneous adsorption	(Gimbert et al. , 2008; Günay et al. , 2007)
Koble–Corrigan	$q_e = \frac{a C_e^{n_k}}{1 + b_k C_e^{n_k}}$	A and b_kKoble–Corrigan isotherm constant;n_kKoble–Corrigan model exponent	• Combination of the Langmuir and Freundlich • Describe heterogeneous surfaces • n_k=1 Langmuir form	(Zhang et al. , 2011)

Table 5. Chemical analysis of Quartz-Albitophire and Metasomatic sample (XRF)

Adsorbent	WT% Component											
	SiO_2	Al_2O_3	Na_2O	Fe_2O_3	CaO	MgO	K_2O	TiO_2	Cl	MnO	P_2O_5	SO_3
Quartz-Albitophire	77.1	10.3	4.59	2.63	1.42	0.77	0.73	0.33	0.071	0.029	0.017	0.018
Metasomatic	50.7	0.18	0.20	12.6	20.4	12.9	0.023	0.105	0.053	0.39	0.070	0.063

Table 6. Arrangement of the CCD forvariables in sulfate adsorption onto Quartz-Albitophire used in the present study.

run	Variable in code levels				Actual value(mg/g)	Predicted value(mg/g)	run	Variable in code levels				Actual value(mg/g)	Predicted value(mg/g)
	x_1	x_2	x_3	x_4				x_1	x_2	x_3	x_4		
1	10	240	200	7	0.19	0.84	16	1.6	130	1100	4	4.25	6.30
2	6	130	2090	4	15.42	17.22	17	2	240	2000	7	11.34	12.18
3	10	240	200	1	1.25	3.63	18	6	130	1100	4	4.95	4.13
4	6	251	1100	4	5.80	4.47	19	2	20	2000	1	30.81	29.08
5	10	20	2000	7	7.14	6.38	20	6	130	1100	0.7	8.58	10.20
6	10	20	200	1	2.59	0.67	21	10.4	130	1100	4	2.60	1.80
7	6	130	1100	4	4.91	4.13	22	6	130	1100	4	4.73	4.13
8	10	240	2000	1	24.32	21.68	23	6	130	1100	4	4.35	4.13
9	2	20	2000	7	17.67	15.66	24	6	130	1100	7.3	1.64	1.29
10	6	130	1100	4	5.07	4.13	25	6	130	110	4	0.47	-0.13
11	2	20	200	1	3.60	3.20	26	10	20	200	7	0.31	0.27
12	6	9	1100	4	2.17	4.75	27	6	130	1100	4	4.79	4.13
13	10	240	2000	7	5.75	6.52	28	2	240	200	1	2.86	2.542
14	2	240	200	7	0.46	-0.88	29	2	240	2000	1	27.57	27.98
15	2	20	200	7	0.59	2.16	30	10	20	2000	1	17.43	19.15

Table 7. Arrangement of the CCD for variables in sulfate adsorption onto metasomatic used in the present study.

run	Variable in code levels				Actual value(mg/g)	Predicted value(mg/g)	run	Variable in code levels				Actual value(mg/g)	Predicted value(mg/g)
	x_1	x_2	x_3	x_4				x_1	x_2	x_3	x_4		
1	10	100	2000	2	38.09	41.67	16	10	10	2000	2	51.30	47.69
2	2	10	250	2	0.18	2.36	17	6	55	1125	4.5	7.89	7.35
3	6	55	1125	4.5	6.62	7.35	18	10.8	55	1125	4.5	12.08	11.56
4	2	100	250	7	0.16	1.55	19	6	55	1125	4.5	10.02	7.35
5	6	55	1125	7.5	3.22	-0.85	20	10	10	250	7	0.04	3.28
6	10	100	250	2	0.28	-2.67	21	6	55	1125	4.5	9.79	7.35
7	10	10	250	2	0.33	0.99	22	2	100	2000	7	13.07	14.43
8	6	55	1125	4.5	5.24	7.35	23	2	10	250	7	0.12	-1.44
9	6	55	1125	1.5	14.36	19.18	24	10	100	250	7	0.37	3.73
10	6	109	1125	4.5	5.98	7.611	25	10	100	2000	7	16.51	12.09
11	6	55	1125	4.5	6.32	7.35	26	6	1	1125	4.5	10.29	9.41
12	6	55	2175	4.5	22.31	29.41	27	1.2	55	1125	4.5	12.51	13.79
13	10	10	2000	7	13.18	13.99	28	2	10	2000	2	54.92	53.58
14	2	10	2000	7	13.04	13.78	29	2	100	250	2	0.03	1.24
15	6	55	75	4.5	0.00	-6.33	30	2	100	2000	2	55.59	50.12

Table 8. ANOVA Table for Experimental design for sulfate adsorption onto Quartz-Albitophire.

Source	Sum of Squares	df	Mean Square	F-Value	p-value Prob> F
Model	1953.34	14	139.52	37.52	< 0.0001
A-pH	77.22	1	77.22	20.77	0.0004
B-t	0.31	1	0.31	0.084	0.7755
C-C0	1167.35	1	1167.35	313.93	< 0.0001
D-m	302.19	1	302.19	81.27	< 0.0001
AB	13.10	1	13.10	3.52	0.0801
AC	54.73	1	54.73	14.72	0.0016
AD	0.41	1	0.41	0.11	0.7431
BC	0.19	1	0.19	0.051	0.8250
BD	5.69	1	5.69	1.53	0.2352
CD	153.07	1	153.07	41.17	< 0.0001
A^2	0.016	1	0.016	4.189E-003	0.9492
B^2	0.59	1	0.59	0.16	0.6953
C^2	50.45	1	50.45	13.57	0.0022
D^2	6.65	1	6.65	1.79	0.2011
Residual	55.78	15	3.72		
Lack of Fit	55.46	10	5.55	88.58	< 0.0001
Pure Error	0.31	5	0.063		
Cor Total	2009.12	29			

Standard deviation	1.93
Mean	7.46
R-Squared	0.9722
Adj R-Squared	0.9463
Pred R-Squared	0.8242
Adequate precision	22.085
PRESS	353.24
Coefficient of variance (%)	25.85

Table 9. ANOVA Table for Experimental design for sulfate adsorption onto metasomatic.

Source	Sum of Squares	df	Mean Square	F-Value	p-value Prob> F
Model	7316.42	14	522.60	28.30	< 0.0001
A-pH	16.27	1	16.27	0.88	0.3628
B-t	10.68	1	10.68	0.58	0.4589
C-C0	4180.76	1	4180.76	226.38	< 0.0001
D-m	1315.56	1	1315.56	71.24	< 0.0001
AB	6.50	1	6.50	0.35	0.5618
AC	20.40	1	20.40	1.10	0.3099
AD	37.29	1	37.29	2.02	0.1758
BC	5.49	1	5.49	0.30	0.5937
BD	16.97	1	16.97	0.92	0.3530
CD	1295.70	1	1295.70	70.16	< 0.0001
A^2	70.91	1	70.91	3.84	0.0689
B^2	3.40	1	3.40	0.18	0.6742
C^2	43.70	1	43.70	2.37	0.1448
D^2	8.24	1	8.24	0.45	0.5143
Residual	277.01	15	18.47		
Lack of Fit	258.09	10	25.81	6.82	0.0234
Pure Error	18.92	5	3.78		
Cor Total	7593.44	29			

Standard deviation	4.30
Mean	12.80
R-Squared	0.9635
Adj R-Squared	0.9295
Pred R-Squared	0.7968
Adequate precision	19.709
PRESS	1543.34
Coefficient of variance (%)	33.57

Table 10. Isotherm model constants for sulfate adsorption onto Quartz-Albitophire and Metasomatic.

	model	parameter	Quartz-Albitophire	Metasomatic
Two parameter models	Langmuir	q_m(mg/g)	24.87	28.50
		R^2	0.9379	0.9227
		R_L	0.77-0.44	0.7155-0.4917
		K_L	2.9613e-04	3.9748e-04
		MPSD	2.140584	0.026214
		RMSE	1.0341	0.916608
		APE (%)	10.69456	7.293418
	Freundlich	$K_F(mg^{1-1/n} L^{1/n} g^{-1})$	0.0671	0.0878
		n(g/L)	1.5524	1.5280
		R^2	0.9016	0.9498
		MPSD	1.137029	0.016112
		RMSE	1.2699	0.738603
		APE (%)	10.55901	5.875083
	Temkin	B_T(KJ/mol)	0.420	0.446
		A_T(L/mg)	0.0025	0.004519
		R^2	0.9660	0.8921
		MPSD	0.732046	0.030267
		RMSE	0.9107	1.082421
		APE (%)	7.016581	8.564477
	Dubinin-Radushkevich	q_m(mg/g)	12.88	12.43
		E(KJ/mol)	5	7.07106
		R^2	0.9799	0.7203
		MPSD	1.712049	0.073428
		RMSE	1.279	1.743111
		APE (%)	10.16698	13.50635
Three parameter models	Redlich-Peterson	K_{RP}	0.0057	0.0097
		a_{RP}	0.1527	0.1513
		g	0.1277	0.1259
		R^2	0.7546	0.7727
		MPSD	1.799298	0.09613
		RMSE	1.6507	1.571223
		APE (%)	10.66286	11.68306
	Toth	q_m(mg/g)	11.98	0.02
		b_T	4.2385e-04	-524.6359
		n_T	0.0803	5.0890
		R^2	0.9960	0.9799
		MPSD	1.321664	0.004279
		RMSE	1.1624	0.467399
		APE (%)	7.448883	2.876284
	Koble–Corrigan	a	0.0324	0.6989
		b_k	8.7807e-04	3.454e-04
		n_k	0.7794	0.1208
		R^2	0.9144	0.9804
		MPSD	3.27415636	0.007063
		RMSE	1.1395	0.461257
		APE (%)	12.19749115	3.549

Table 11. The amount of sulfate adsorption in water wells of Bafq district.

Wells	pH	EC (mS/cm)	TDS (g/l)	Cl^- (mg/l)	SO_4^{2-} (mg/l)	Ads.(mg/g)	
						Metasomatic	Quartz-Albitophire
No.1 (Sadrabad well)	7.14	11.87	5.94	439.20	962.60	4.524352	2.169722
No.2 (Bagherabad well)	7.88	84.6	4.32	2061.40	600	1.878734	1.165823
No.3 (Ghavidel well)	7.16	29	14.51	3646.20	1886	29.33484	15.62129
No.4 (Slamabad well)	7.28	29.7	14.83	4119.90	1636	15.55226	10.92

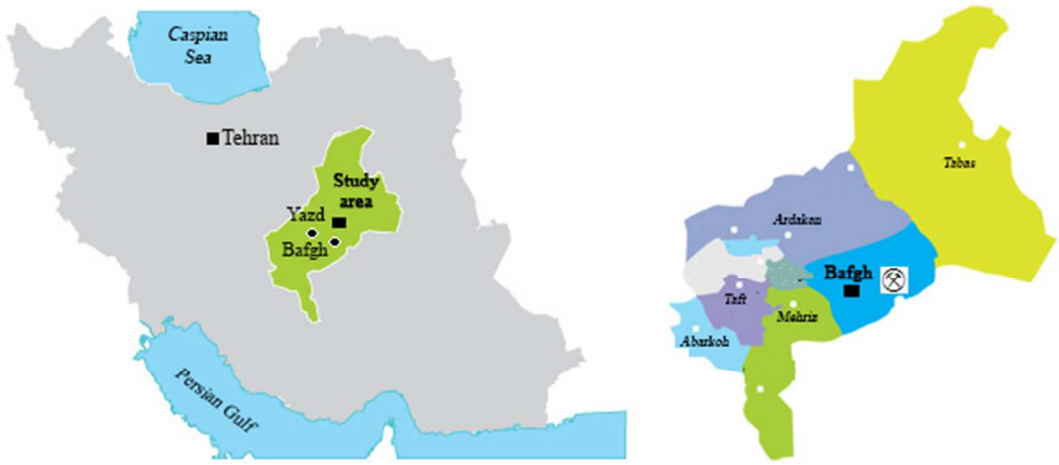

Fig. 1. The map of study area.

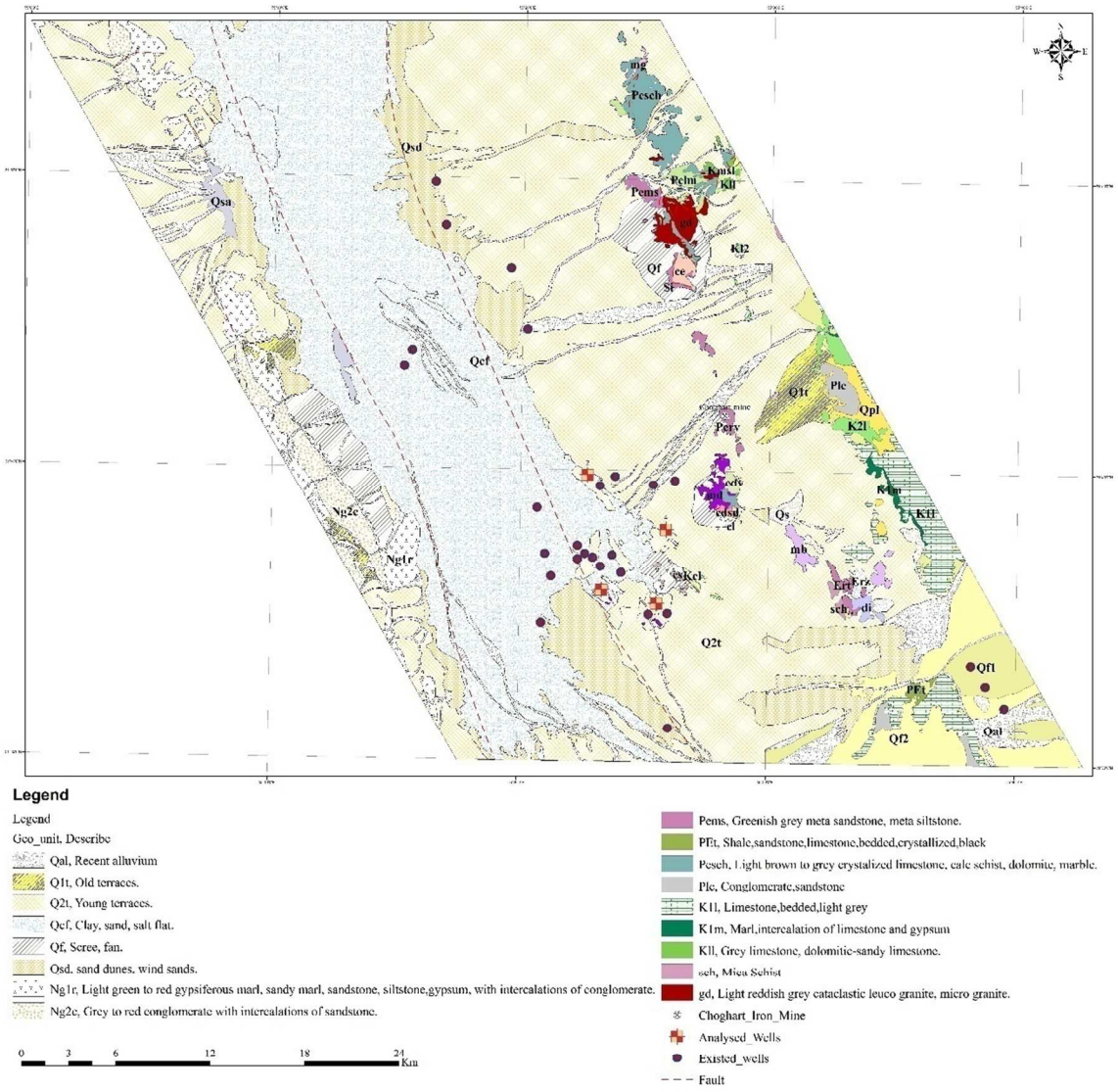

Fig. 2. The map depicts study area in center of Iran and the location of Choghart mine and water wells in the area.

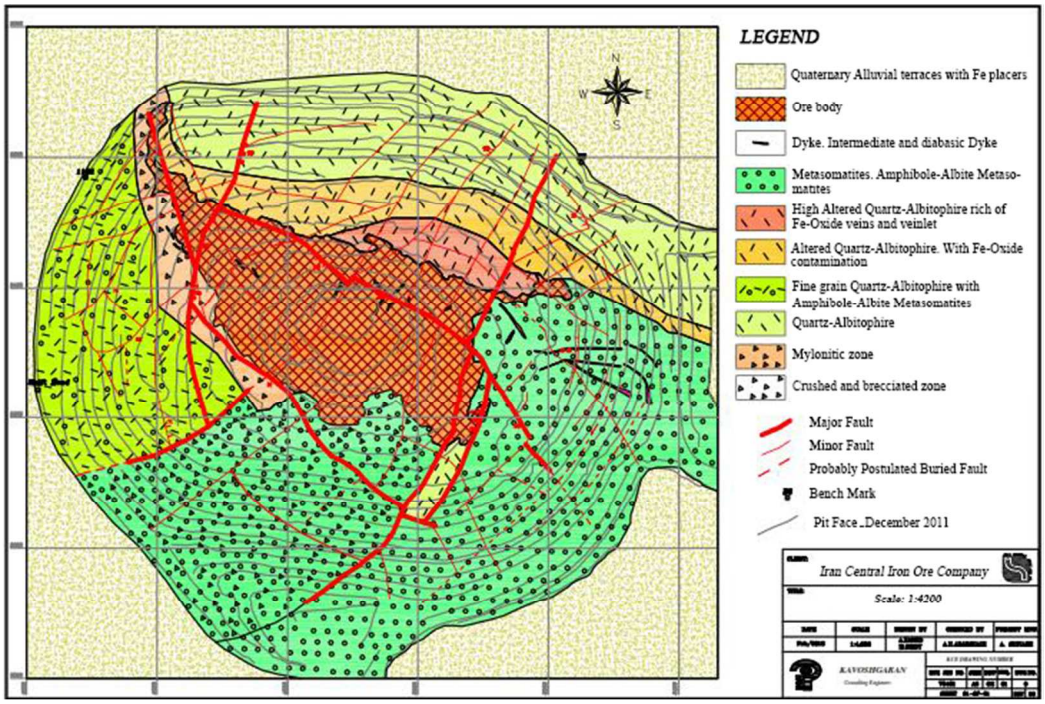

Fig.3. Simplified geological map of the ore body of the Choghart deposit (pit face 2011).

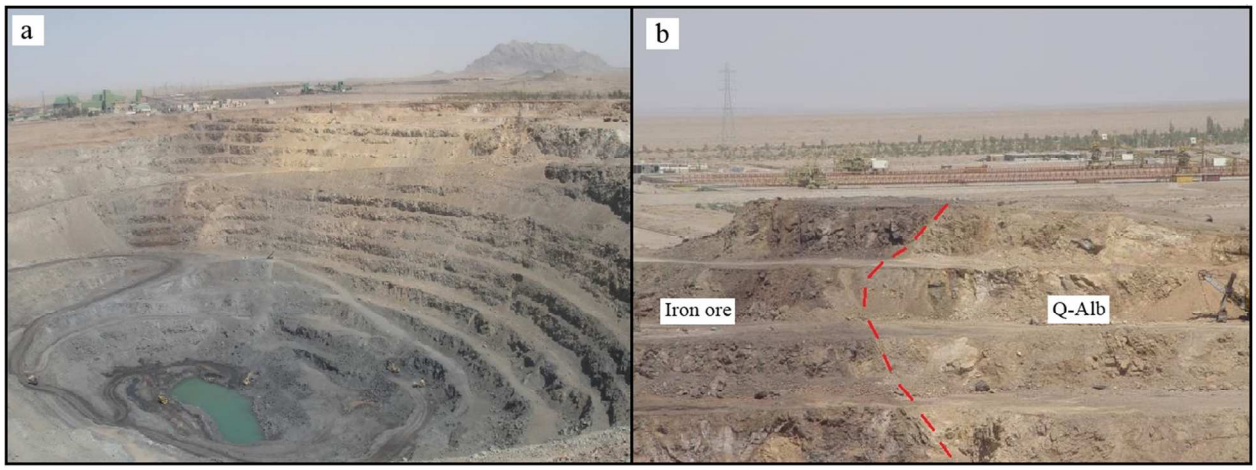

Fig. 4. The Choghart iron deposit. a A panorama showing part of the north eastern ore body. b Sharp contact between the Quartz-Albitophire (Altered rhyolite) host rock and the iron ore.

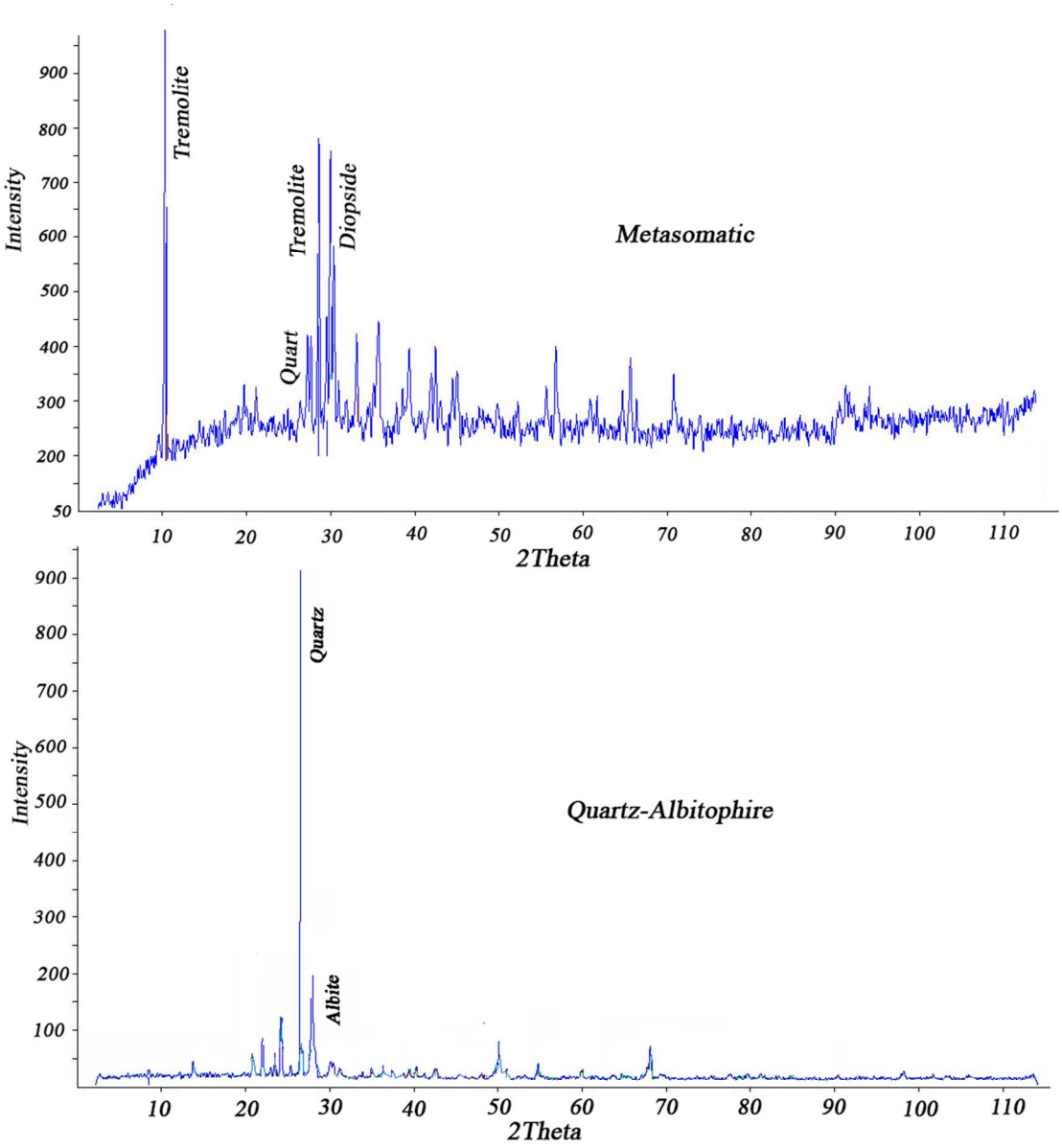

Fig. 5. XRD pattern of Quartz-Albitophire and Metasomatic.

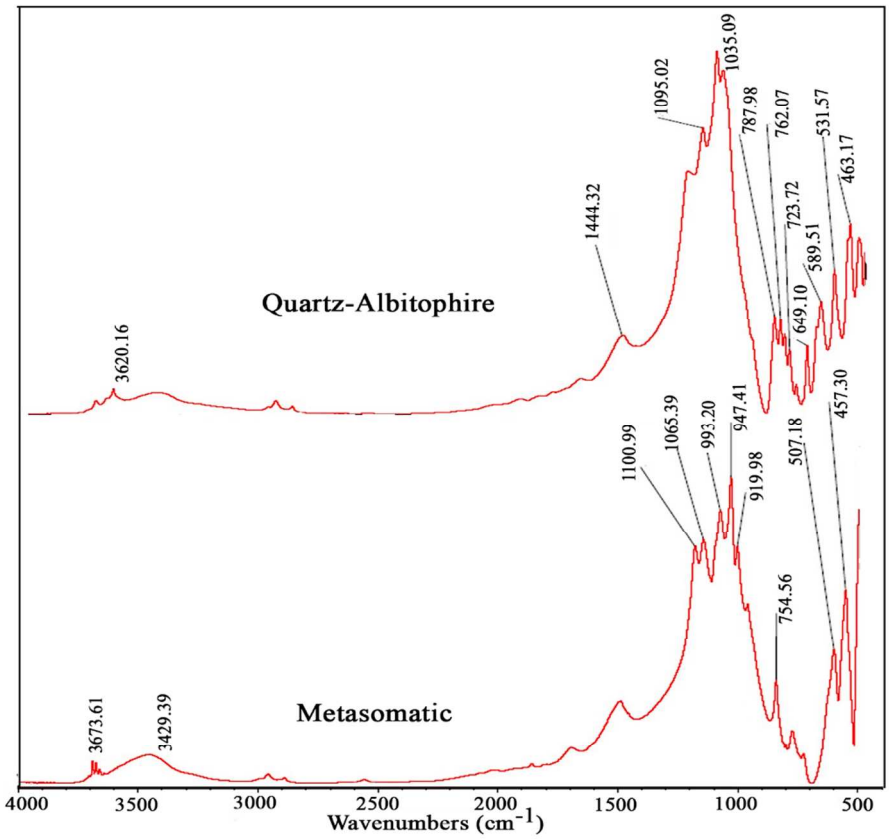

Fig. 6. FTIR spectra of Quartz-Albitophire and Metasomatic samples.

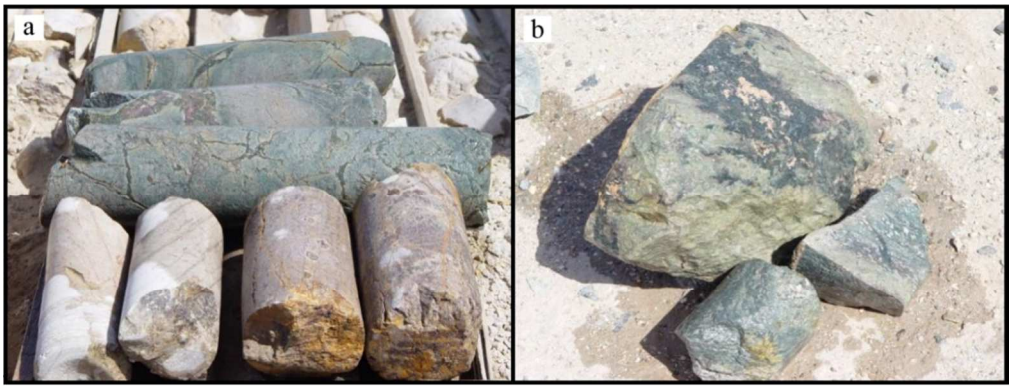

Fig. 7. The Choghartiron waste rocks. A Quartz-Albitophire and altered rhyolite in bright color and metasomatic in green color. b metasomatic rocks.

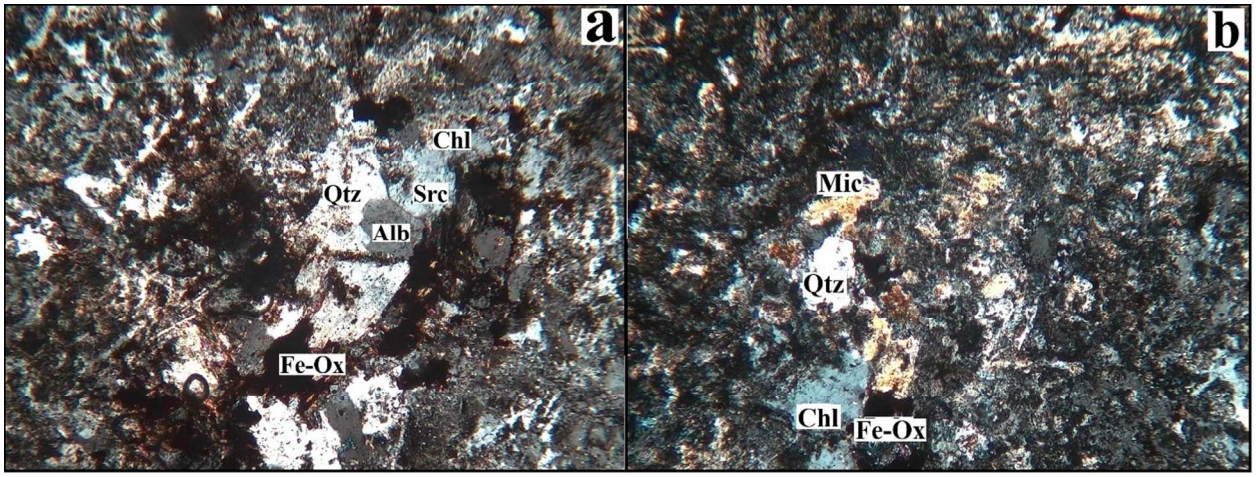

Fig. 8.Photomicrographs of Quartz-Albitophire host rockin thin section (XPL).(Chl: Chlorite, Qtz: Quartz, Src: Sericite, Alb: Albite, Fe-Ox: iron oxide, Mic: mica)(50x)

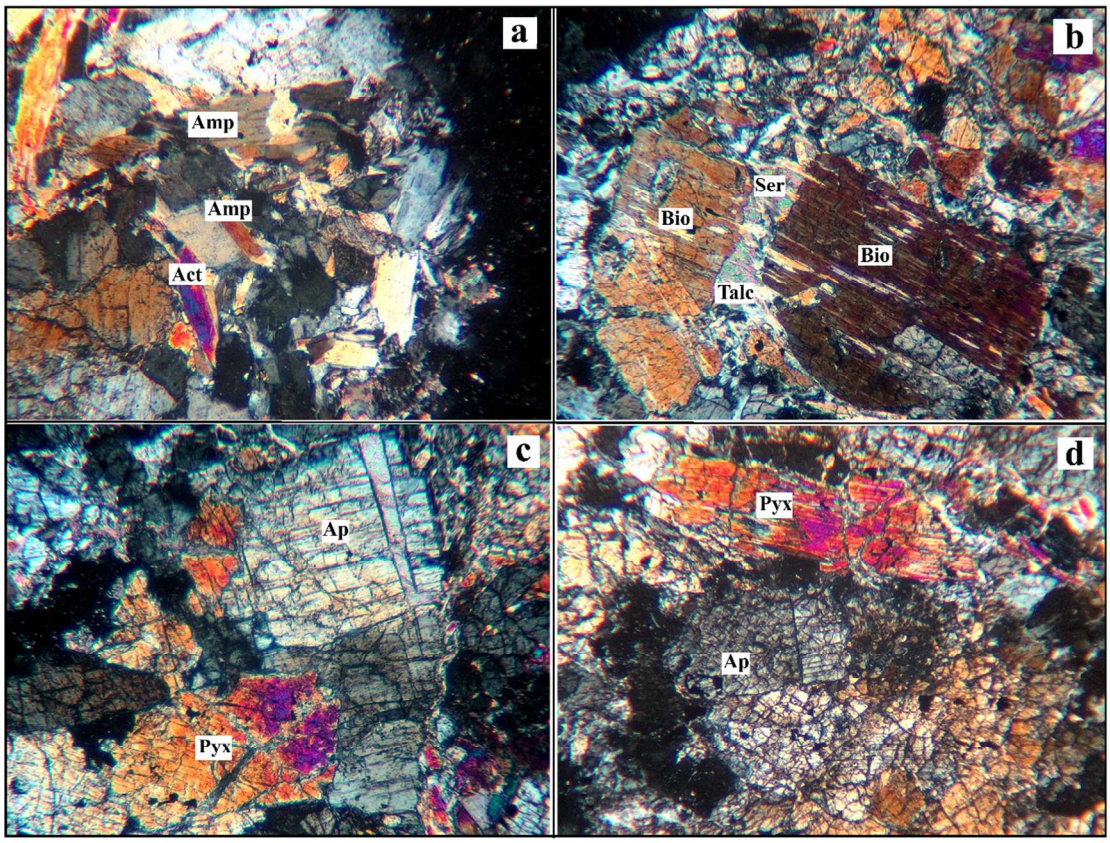

Fig. 9.Photomicrographs of Metasomatic host rock in thin section (XPL). A Actinolitization in the host metasomatic. b Talc-Serpentine and Biotite in host metasomatite. c,dApatite and pyroxene in host rock. (Act: actinolite; Bio: Biotite; Ser: Serpentine; Pyx: Pyroxene;Ap: apatite). (100X)

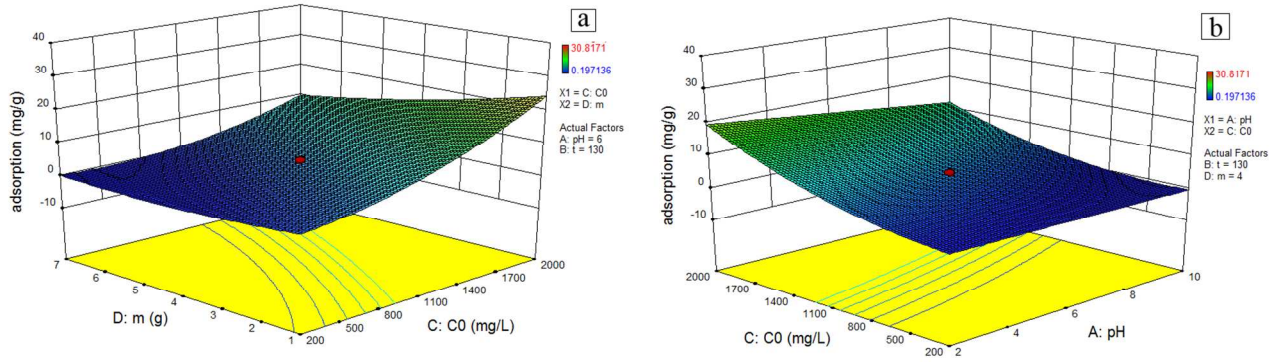

Fig. 10.Surface plot of the effects of main variable interaction on the sulfate adsorption onto Quartz-Albitophire, a. Sulfate initial concentration and amount of Quartz-Albitophire, b. sulfate initial concentration and pH

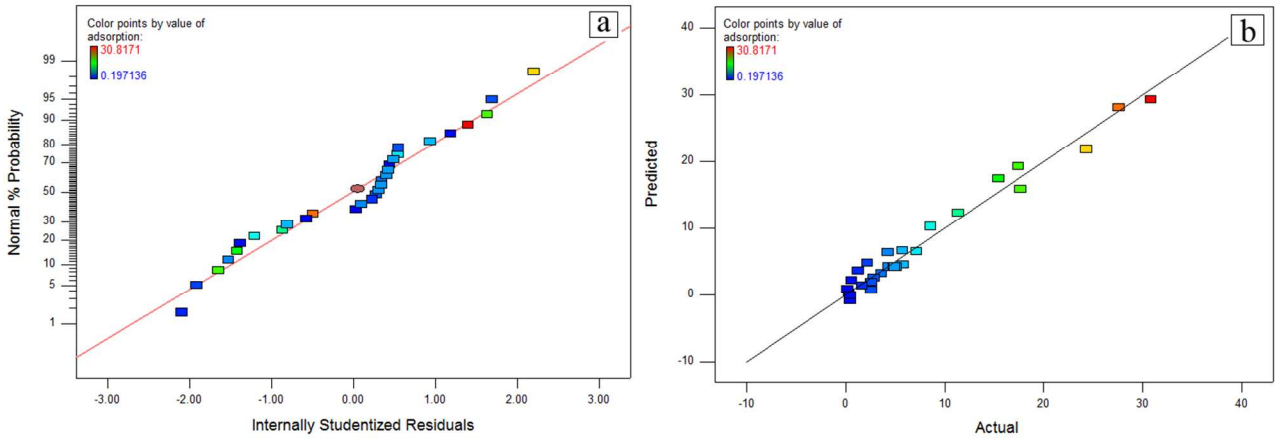

Fig. 11. A. Normal plot of residual for sulfate removal; b. Relation between experimental and predicted sulfate removal by Quartz-Albitophire.

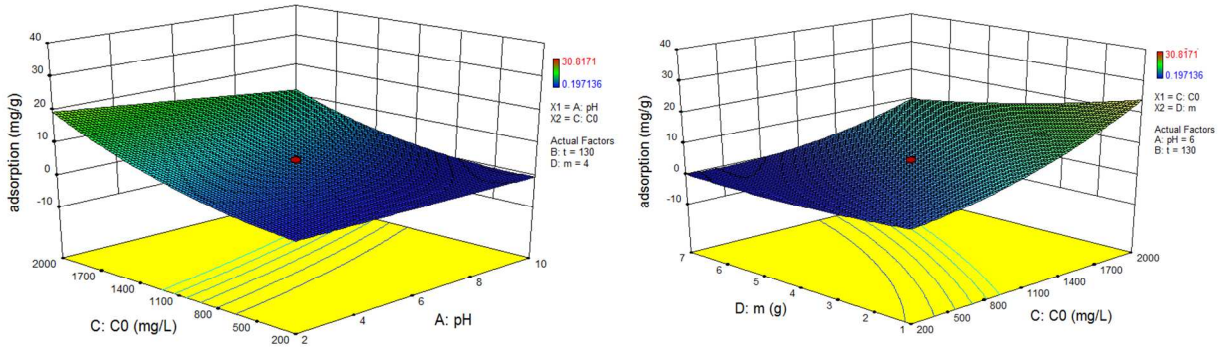

Fig. 12. Surface plot of sulfate adsorption onto metasomatic showing interaction between sulfate initial concentration, pH and amount of metasomatic at the central values of other parameters.

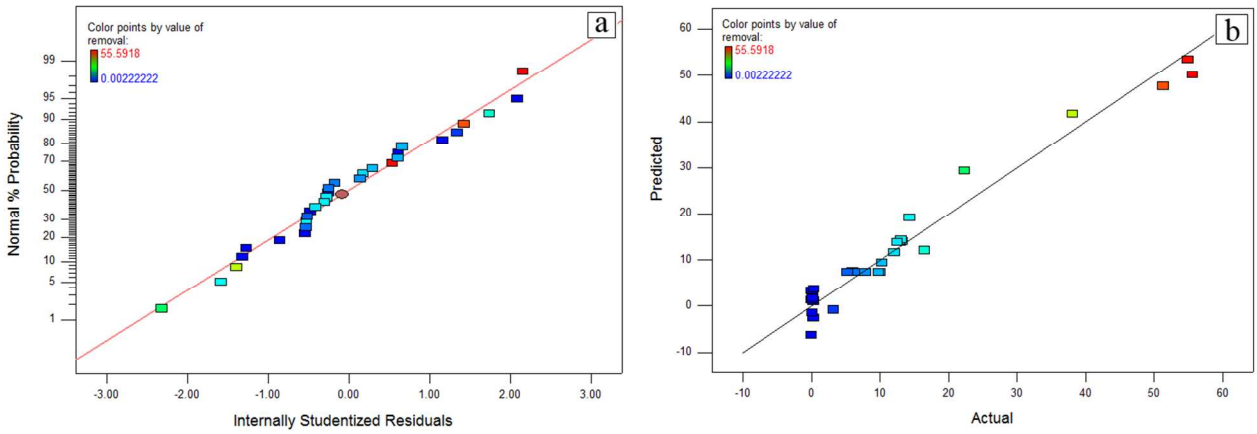

Fig. 13. a. Normal plot of residual for sulfate removal,; b. Relation between experimental and predicted sulfate removal by metasomatic.

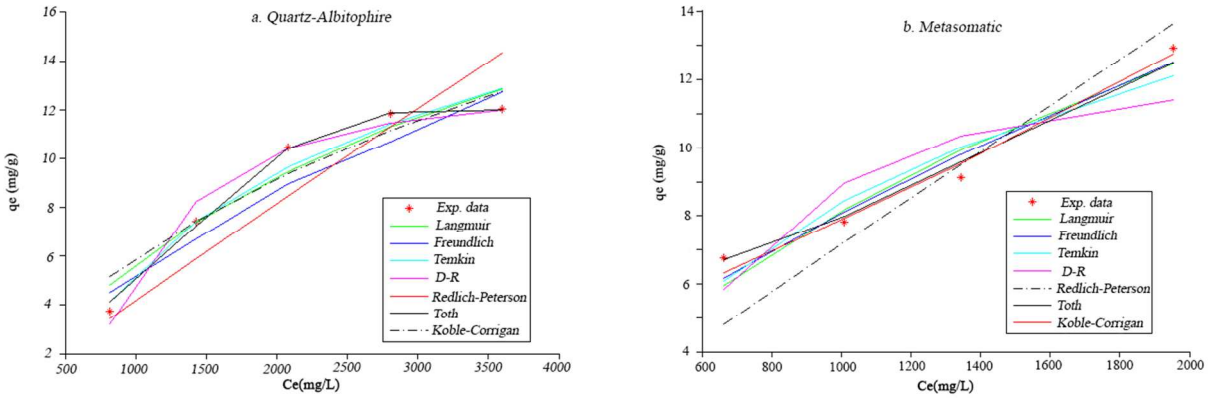

Fig. 14. Isotherm plots for sulfate adsorption onto a. Quartz-Albitophire and b. Metasomatic.